Physiologically Based Modeling of 3-D Vascular Networks and CT Scan Angiography

Marek Kretowski, Yan Rolland, Johanne Bézy-Wendling*, and Jean-Louis Coatrieux, *Fellow, IEEE*

***Abstract*—In this paper, a model-based approach to medical image analysis is presented. It is aimed at understanding the influence of the physiological (related to tissue) and physical (related to image modality) processes underlying the image content. This methodology is exemplified by modeling first, the liver and its vascular network, and second, the standard computed tomography (CT) scan acquisition.**

After a brief survey on vascular modeling literature, a new method, aimed at the generation of growing three-dimensional vascular structures perfusing the tissue, is described. A solution is proposed in order to avoid intersections among vessels belonging to arterial and/or venous trees, which are physiologically connected. Then it is shown how the propagation of contrast material leads to simulate time-dependent sequences of enhanced liver CT slices.

***Index Terms*—Computed tomography (CT), hepatic enhancement, image simulation, physiologically based modeling, vascular network.**

I. Introduction

THE last decades brought significant progresses in medical imaging, especially with the improvement of new devices like CT, magnetic resonance imaging (MRI), and ultrasound (US). These imaging modalities play an essential role for diagnosis. However, it must be recognized that medical images are still visually explored by the radiologists. This visual analysis takes into account *a priori* knowledge related to anatomy and physiopathology of the tissues and the organs without providing reproducible, robust, objective measurements capable to quantify the extent of a disease and to follow-up its evolution. These limits have motivated the design of automatic methods aimed at image characterization (texture analysis for instance [1]). Even if the capability to provide precise quantifications can be assessed by these methods, they often remain at a descriptive level and do not establish any link with the physiological processes underlying the observed patterns. In other words, the image interpretation often stays at a surface level instead of relying on physiological mechanisms and variables. The objective of this contribution is to show how a model-based approach can relate external descriptions to the internal processes or systemic behaviors, which originate them. This approach belongs to the field of computational modeling that addresses the simulation of complex biological objects. The organ model includes both structural and functional properties as well as growth and pathological evolutions. To be of relevance, the acquisition modality has to be modeled as well, in order to understand what is exactly represented in the image. This model-based method is illustrated on vascular structures whose changes (related to structure, geometry and function) lead to pathological situations or, conversely, whose changes are directly induced by diseases (like tumor, hypertension, diabetes). Most of these modifications appear on medical images, especially when acquisition is done after injection of a contrast material (CM), which enhances the vascular network.

The simulation of vascular variations (from normal to pathological) and imaging parameter configurations will allow to examine their influence on the image characteristics, like for instance textural features. More precisely, a three-dimensional (3-D) model of connected vascular trees (i.e., veins and arteries) has been developed and is coupled with a CT scan acquisition model, based on a standard reconstruction algorithm.

The remaining parts of this paper are organized as follows. Section II describes the different steps of the model-based approach of image analysis. Section III briefly reports a state of the art in vascular modeling. Section IV provides a description of the proposed organ model while it is shown in Section V how the model can be applied to simulate CT scan images. Experimental results are displayed in Section VI. Discussions and some plans for future research are sketched in Section VII.

II. Model-Based Approach to Image Analysis

The methodology we adopt is depicted in Fig. 1. The *virtual space* is made of all the modeling steps, and the *physical space* is constituted of corresponding real processes. The real and virtual outcomes can be compared, either at a visual level or through quantitative characteristics. For example, local and global statistical measures can be performed on the simulated as well as on the real images, which can bring new cues for model building and adjustment (initialization conditions, error criteria,…). Similar feature extraction (distances, volumes, and shape descriptors,…) can be achieved into the image planes issued from virtual and physical imaging devices.

The modeling part is organized in four successive levels: object → sensor → image → decision. In the object space, the

Manuscript received August 23, 2002; revised October 24, 2002. The Associate Editor responsible for coordinating the review of this paper and recommending its publication was J. Liang. *Asterisk indicates corresponding author.*

M. Kretowski is with the Department of Computer Science, Technical University of Bialystok, 15-351 Bialystok, Poland, and LTSI, INSERM, University of Rennes 1, 35042 Rennes, Cedex, France.

Y. Rolland is with the Department of Radiology and Image Processing of the South Hospital of Rennes, Rennes, France, and LTSI, INSERM, University of Rennes 1, 35042 Rennes, Cedex, France.

*J. Bézy-Wendling is with the LTSI, INSERM, University of Rennes 1, B. 22, Campus of Beaulieu, 35042 Rennes Cedex, France (e-mail: johanne.bezy@univ-rennes1.fr).

J.-L. Coatrieux is with the LTSI, INSERM, University of Rennes 1, 35042 Rennes, Cedex, France.

Digital Object Identifier 10.1109/TMI.2002.808357

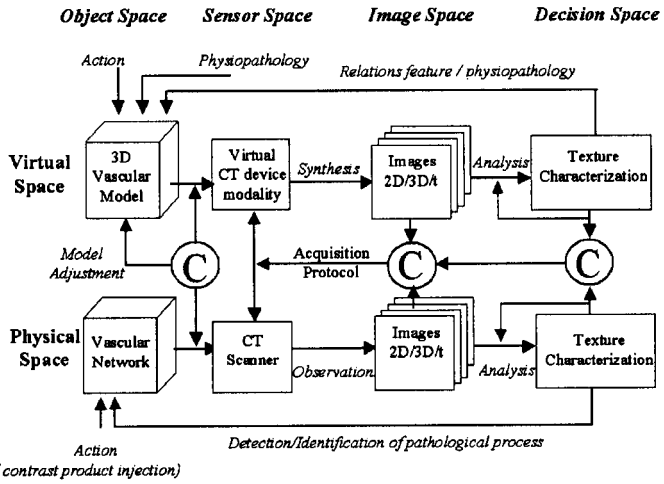

Fig. 1. Model-based approach for angiographic image analysis. Vascular networks, CT scanner, 3-D+t images, and textural discrimination are depicted. This particular situation can evolve by changing the organ, the imaging modality and the image processing tools, offering a wide spectrum of potential applications. "C" means comparison between real and virtual outcomes at each step of the methodology.

basic mechanisms originating the organ and its vascularization, the environmental conditions in which they develop (i.e., functional interactions and spatial constraints for instance) and the deviations that can occur during their formation or after (reflecting interindividual variations as well as pathological evolutions) are taken into account. In the sensor space, the physical principles of CT acquisition are modeled. The main acquisition parameters can be changed, leading to a set of images with varying slice thickness, resolution, and acquisition time after CM injection. Finally, such simulated images can be characterized, by texture analysis methods for instance, and linear or nonlinear relations between the textural features and the underlying, fully controlled, physiological variables can be estimated. This way, this model-based approach allows to link the extracted features to relevant pathophysiological patterns, leading to replace formal parameters by variables with a structural or functional meaning. Moreover, the influence of the acquisition parameters on the image characteristics can be objectively anticipated, and the performances of image analysis methods for detection and characterization can be assessed.

This scheme could certainly be extended to more generic situations, where the *object* would be any organ or biological tissue, the *sensor* any imaging device, and where the synthesized *images* could be analyzed in order to take a *decision* regarding potential disorders based on morphological, structural, or functional characteristics of the organ.

III. Background on Vascular Modeling

A few approaches to vascular tree modeling have been proposed so far. They can be classified in different categories, according to various characteristics like organ, level of details, or application. Here, they are grouped following a very significant geometrical feature, the dimensional space in which they are represented. The two-dimensional (2-D) models are, therefore, first introduced, and then the 3-D models are described.

A. Two-Dimensional Models

Gottlieb [2] and Nekka [3] proposed physiologically based models of growing vascular trees where tissue growth combined with biological rules of angiogenesis lead to a the development of new vessels, but vascular patterns are too schematic when compared with the natural vascular networks. Recently, Meier [4] proposed another physiologically based model for the automatic generation of vascular structures relying on the surface of an arbitrary abdominal organ. The method was aimed at improving the virtual rendering of laparoscopic images. All these attempts do not include any hemodynamic feature (flow, pressure).

In [5], Schreiner and Buxbaum reported the method called "constrained constructive optimization" (CCO) for modeling an arterial tree. In this approach, regions that are not yet perfused are randomly chosen in a 2-D circular area representing the perfusion surface, and these regions are successively supplied by new segments. A new bifurcation is optimized geometrically, considering a particular target function, and then the whole tree is re-scaled to meet boundary physiological conditions (pressure and blood flow). The symmetry properties of coronary vascular trees simulated by CCO are presented in [6] and it is shown in [7] that different structures of coronary vascular trees obtained by CCO lead to the same functional performances.

The work of Anderson and Chaplain [8] presents a low-level approach to tumor-induced angiogenesis. The authors developed both continuous and discrete mathematical models, which describe the formation of the capillary sprout network in response to chemical stimuli [tumor angiogenic factor (AF)] supplied by a solid tumor.

B. Three-Dimensional Models

In [9] and [10], Lefevre studied the relation between the fractal complexity of pulmonary arterial trees, the way they develop (angiogenesis), and their hemodynamic efficiency (small arterial volume, fast adaptation to varying metabolic needs), but no geometric representation of the resulting vascular trees is given.

Glenny and Robertson [11] developed a very simple branching model of a pulmonary vascular tree to study regional perfusion. The vessels branch along one of the three orthogonal directions to assure a space-filing structure. The main variables deal with the blood flow asymmetry and the effect of gravity at each bifurcation. A more advanced model of a pulmonary arterial tree was proposed by Parker *et al.* [12]. In addition to the parameters used in [11], the branch angle, mother-daughter length ratio and branch rotation angle are defined for a single bifurcation. Even if flows produced by both models were similar to natural ones, the geometry of the simulated trees is still simplified (too regular, clearly artificial) in comparison to natural structures.

Karch *et al.* [13] extended the CCO method to simulate coronary arterial tree within a convex 3-D piece of tissue, including terminal flow variability. In [14], the authors combined their method with the staged growth of the tissue: a sequence of vascular growth domains is defined by means of a probability density function, varying with time. This variation of conventional CCO leads to structural variations inside the vascular tree, and was applied to simulate a thin tissue layer parallel to the epicardiac surface, containing the main vascular branches, and which

progressively extends to the endocardiac surface. However, the growth of vessels was not taken into account in these models. In fact, existing vessels are part of the tissue and they should grow synchronously with the tissue. Moreover, the simulated vascular trees were truncated, at the prearteriolar level.

These several contributions have highlighted the inherent difficulties to derive physiologically sound models. If they provide new means to simulate vessel networks, they remain at a descriptive representation level, a subjective comparison being performed to evaluate their capability to match real data. To our knowledge, none of the previous models was used in order to realistically generate medical images which has been our primary objective.

Our own work, earlier reported in [15], allowed to simulate the growth of a vascular tree in a 3-D simple shaped volume. In [16], this model has been used to simulate structural and geometrical variations of the vascular tree, induced by local changes of the vascular density, the local blood flow, and the rate of cells proliferation. These vascular modifications were illustrated by the simulation of an hypervascular region in the liver, corresponding to a tumoral process. This model was used to simulate the appearance of vessels in medical slice images [17], with a simplified geometrically based method for the image formation. A more realistic model of CT has been later proposed [18], and the influence of the slice thickness on textural features was assessed.

In this paper, new advances concerning the vascular model as well as the CT scan simulation are presented. They mainly deal with the global growth of the whole organ and the vessels at each cycle, the algorithm used to avoid any crossing in one tree or between multiple trees, the hemodynamic connections between two trees (as opposed to the geometrically connections like those reported before), and the CT simulation of the vessels enhancement at different times after injection of CM.

IV. Model Description

In its generic form, the model is designed to simulate the development (and/or pathological changes) of a given extensive organ, in which all cells are able to divide all along their life, allowing the organ to increase its size [19]. It consists of two main components: the tissue and the vascular network that perfuses it, and adapts to its local geometry. The process starts with an organ (here, the liver), whose size is a small fraction of the one of an adult organ, and continues until it reaches its full size. The changes in the size and structure of the organ and the corresponding vascular trees operate at discrete time instants called cycles (and subcycles). The overall flow chart (Fig. 2) depicts the main events, which can be distinguished in the model realization of the organ development process. These steps are described in the following sections.

A. Tissue Modeling

Simulations of the tissue growth are carried out in an istropic 3-D array of computational sites defining the organ shape. These sites, evenly distributed in the organ, define the potential locations for macro-cells inside the bounding shape. Each macro-cell is a small, fixed size part of the tissue, and constitutes the functional unit of the model. It is characterized by its class, which determines most of functional/structural (e.g., minimal distance between macro-cells: *MinDist*, probability of mitosis/necrosis: Pb_m/Pb_n) and physiological features (e.g., blood flow rate or corresponding pressures). Several classes of macro-cells can be defined to differentiate functional (or pathological) regions of tissue. Furthermore, certain parameters, associated with the macro-cell class, are described by their distribution and they are randomly chosen (around a mean value) for each new macro-cell. For example, the variability of the terminal blood flow (in macro-cells) is taken into account in the model based on

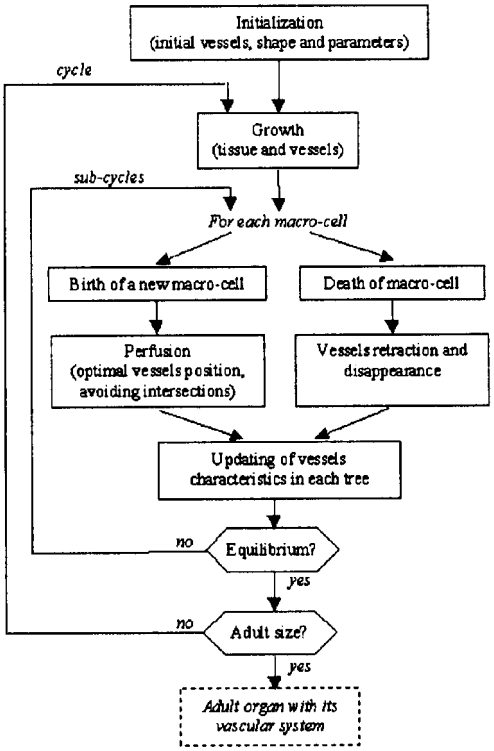

Fig. 2. Flow chart representing two loops of events which are distinguished in modeling of the organ (tissue and vascular network) development.

$$Q_i = f\left(Q_\mu, Q_\sigma\right) \tag{1}$$

where Q_i is the blood flow rate for ith macro-cell; $Q\mu$ and $Q\sigma$ are the blood flow average and standard deviation, respectively, and f is a function which adds a value situated between $-Q\sigma$ and $Q\sigma$ to $Q\mu$.

The organ growth results of either *hyperplasia* (increase of the number of structural units) or *hypertrophy* (increase of their size) [19]. In the model, the size of macro-cells remains unchanged; hence, the development of tissue results from hyperplasia.

To simulate the development of an organ, the external shape expands periodically (at cycles) until the organ reaches its adult size. The relative positions of macro-cells inside the tissue remain unchanged, but distances between macro-cells increase, leading to the apparition of empty spaces. These spaces are then filled by new macro-cells in consecutive subcycles. Subcycles are repeated until the equilibrium is reached between the number of new macro-cells and the number of dying ones. In

each subcycle, a macro-cell can divide into two daughter macro-cells of the same class (probability of mitosis, Pb_m). The new macro-cell position is chosen randomly in the neighborhood of the "mother" (not closer that *MinDist* and not farther than *MaxDist*) but created only if the local constraints of maximal density and minimal distance for all macro-cells are fulfilled. The macro-cell can also die according to a given probability (probability of necrosis, Pb_n) which is usually lower than Pb_m especially when the organ is young. Furthermore, probabilities of mitosis/necrosis are sensitive to time and they decrease with the age of macro-cells [19]. More precisely, Pb_m and Pb_n are both described by exponentially decreasing functions

$$Pb_x(t) = x_1 \cdot e^{(-t/x_2)} \tag{2}$$

where $x = \{m, n\}$, t is the cycle number, and $x_i \in [0, 1]$ $(i = \{1, 2\})$ are the corresponding coefficients. This process simulates the natural evolution in which cells regeneration is faster at the beginning of the development $(m_1 > n_1)$, but becomes slower with age, except in particular pathological cases, where it can lead to organ atrophy (anemia).

B. Modeling Vascular Network Perfusing the Tissue

A vascular network represents two vascular trees with blood going from the arterial tree to the venous one through macro-cells (see Fig. 3). The macro-cells correspond to capillaries of real vascular system and they play the main role in the exchange process of oxygen, carbon dioxide and nutrients.

The number of branches at each bifurcation is almost invariably two according to morphometrical investigation conducted by Zamir [20]. Sometimes, *anastomosis* can be observed especially when vessels with very small radii are taken into account. Because it requires transition from the tree to a directed graph structure and much more complicated algorithms to deal with blood flow and optimization, this level of detail has not yet been integrated into the current model. The vascular network is considered as a binary tree (or unary in some specific situations) with nodes characterized by their spatial position, blood flow rate (Q) and pressure (P) (see Fig. 4). Each vessel segment[1] is an ideal tube with a wall thickness depending on the vessel radius and function. Blood is considered as a Newtonian fluid, with constant viscosity (μ), whose flow is governed by *Poiseuille's law*

$$\Delta P = Q \cdot \frac{8 \cdot \mu \cdot l}{\pi \cdot r^4}. \tag{3}$$

This equation is used to calculate the pressure difference between the two extremities of a vessel depending on the blood flow rate (Q), the length (l), and the radius (r) of the vessel. At each bifurcation, the *law of matter preservation* has also to be fulfilled

$$Q = Q_R + Q_L. \tag{4}$$

It gives the relation between blood flows upstream and downstream the bifurcation and states that the quantity of blood, which enters a bifurcation by the mother branch, leaves it by the two daughter branches.

[1]According to Zamir's notion [20] a vessel segment is defined as a part of the vessel between two bifurcations.

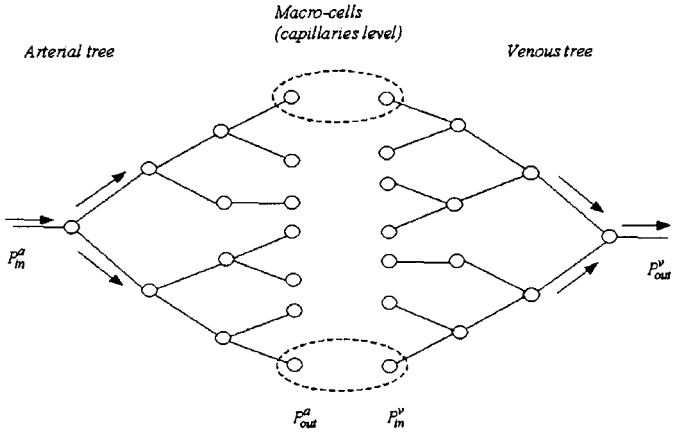

Fig. 3. Two vascular trees connected at the macro-cell level (a macro-cell is a simplified representation of capillaries, where exchanges between blood and tissue take place), $P^{a(v)}_{\text{in(out)}}$—blood pressure at the *input* (*output*) of the *arterial* (*venous*) tree, respectively.

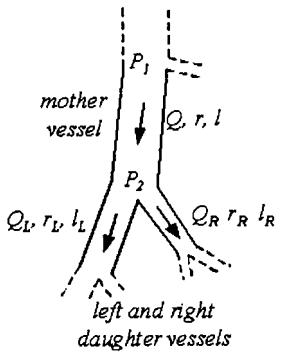

Fig. 4. The binary vascular tree is composed of successive bifurcations. Symbols P, Q, r, and l associated with the mother and daughter vessels correspond, respectively, to blood pressure, blood flow, radius and length.

The decrease in the vessel radii when going from proximal to distal segments of the vascular tree can be observed in any healthy vascular tree. Based on experimental data relation between the radius of the mother vessel (r) and radii of its two daughters (r_L, r_R) can be established

$$r^\gamma = \alpha \cdot r_L^\gamma + \beta \cdot r_R^\gamma. \tag{5}$$

This general form of the *bifurcation law* ([20]–[22]), was confirmed by morphometrical analyzes and theoretical studies. In simpler case, $\alpha = \beta = 1$ and γ varies between 2 and 3, but more complicated equations using blood flow to define α and β were also proposed (e.g., [21]).

The development of vascular network is directed by increasing needs of the growing tissue [20]. New macro-cells are not perfused by the existing vascular system. They signalize this by secreting some AFs, which stimulate the closest vessels to sprout new vessels toward the macro-cell [23]. This process can be seen as a kind of competition, because only one vessel from each tree will perfuse the macro-cell and the remaining vessels will retract and then disappear. The maximal number of vessels, situated in the neighborhood of a new macro-cell, which respond to AF (candidates for perfusion), is one of the simulation parameters. In fact, to perfuse the macro-cell, each candidate vessel creates a new bifurcation and then the optimal branching position is searched (see Fig. 5). It is widely accepted

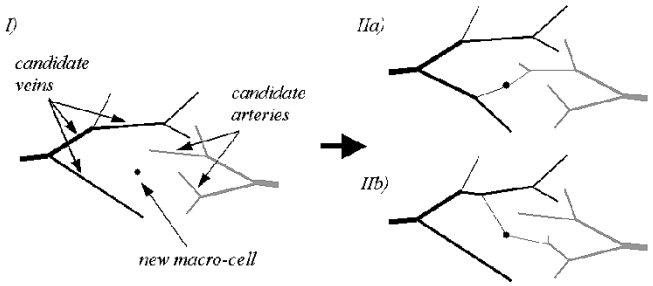

Fig. 5. The closest vessels that respond to AF stimulation are called candidates. Each candidate vessels creates temporarily a new bifurcation and an optimal branching position is searched.

that geometry and organization of vascular trees is governed by some optimality principle ([21], [22], [24], and [25]), but still there is no consensus on what criterion function should be used. The minimal blood volume condition has been chosen here and thus, given the spatial positions (i.e., coordinates and radii) and physiological properties (i.e., blood flow and pressure) of newly created vessels, the optimal bifurcation points are searched using the method proposed in [21] and adapted to the 3-D situation. It has been assumed that, during this local optimization, the influence of moves of the bifurcation point on the remaining vessels is relatively small and can be neglected. Such a simplification allows us to significantly reduce the computational complexity and to simulate highly complex trees in a reasonable time. When the geometry of the bifurcation is known, the next step is devoted to the updating of vessel's characteristics (i.e., blood flow, pressures, and radii) in the whole tree. To perform this in an efficient way, a method called "fast updating" was developed [26]. The result of this optimization process is a tree fulfilling all constraints (i.e., physical and physiological laws). As aforementioned, only one vessel from each tree is designated to perfuse the macro-cell, hence, the best configuration has to be found. For each candidate, the volume of the whole tree is computed and the candidate with the corresponding minimal value is retained.

Unfortunately, it is not enough to perform geometrical optimization to obtain the valid bifurcation position. The problem of avoiding "collision" among vessels has also to be studied, especially in the case of crossing among arteries (arterioles) and veins (venules). In some models (e.g., [3] and [4]), the fusion of vessels from the same tree allows to introduce anastomosis, but such a situation is not expected to occur in the present model. To detect a collision, the procedure based on the computation of the shortest distance between two lines in three dimensions[2] and using radii of vessels can be exploited. It requires to check possible intersections between all vessels at each geometrical change, and the computational cost is high ($O(6 * S^2)$, where S is number of vessel segments in a single tree). More heuristic approaches have to be proposed. When a collision is detected, the subsequent issue to be solved is how to modify the configuration at hands while respecting the overall constraints above described. The simplest method, which has been applied here, consists to eliminate, among the all candidate solutions, the nonfeasible ones. This issue is omitted in the literature mentioned so far and is even more complicated as soon as the growth process

[2]Corresponding equations can be found on P. Bourke web page.

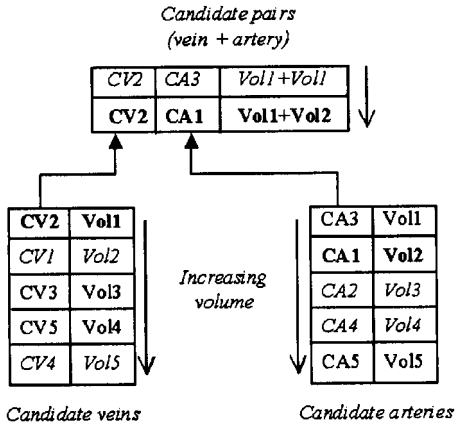

Fig. 6. Selection of the minimal volume, nonintersecting configuration of vessels, for the perfusion of a new macro-cell. Rows in candidate tables correspond to optimal bifurcation positions found for each candidate and detected collisions are marked in *italic*.

is considered. More sophisticated procedures of passing (or correcting) must be designed.

Consequently, the avoidance of possible intersections of vessels when searching for optimal bifurcation positions in arterial and venous trees should be looked for. In our model, the problem was solved as follows (see, also, Fig. 6).

1) The candidate vessels, which respond to AF secreted by a new macro-cell in each tree, are identified (N-number of candidate vessels).
2) Each candidate is used to temporarily perfuse the macro-cell; the resulting bifurcation is optimized and the corresponding volume is computed and stored (with the bifurcation configuration).
3) Collisions (if any) are detected inside each tree and some candidates are eliminated (2 trees $*N$ candidates $*$ 3 vessels in bifurcation $*(N-1)$ remaining candidates $= 6N(N-1)$ checks).
4) The candidates are sorted according to increasing volume.
5) The pair of candidates with the lowest sum of volumes is chosen; the possible crossing between vessels from opposite trees is checked.

— Vessels constituting the bifurcation in the first tree can intersect with vessels creating the bifurcation in the second one (except those directly connected to the macro-cell) (8 checks).

— Vessels constituting the bifurcation in the first tree can intersect with other candidate vessels in the second tree (2 trees $*$ 3 vessels $*(N-1)$ candidates $= 6(N-1)$).

6 When the collision is detected, the next pair of candidates (with the second lowest volume) is tested [see 5) above] and so on, until the suitable configuration is found.

7 If the proper pair is found, the candidates are used to permanently perfuse the macro-cell by vascular system; otherwise the macro-cell dies.

A configuration of a new macro-cell and surrounding vessels, in which the model is not able to perfuse this macro-cell (because of possible intersections among perfusing vessels), is rare, but may happen. This phenomenon can be explained by

the simplified vessel's representation as a rigid straight tube between bifurcations, while in reality the vessels are elastic and can easier adapt to the local situation. If we try to overcome the above problem by increasing too much the number of candidate vessels, it can lead to an artificial configuration, when the macro-cell is perfused by too distant vessels.

As it has been already mentioned, macro-cells can also die (with probability Pb_n at each growth subcycle). In that case, two vessels supplying the macro-cell retract and disappear. The corresponding bifurcation is reduced to two segments connected at the former bifurcation point. In order to minimize the blood volume, such a configuration of vessels can be replaced by a single straight vessel if, and only if, no intersection is detected. This is why in some situations the binary tree has to be replaced by an unary one.

V. Medical Image Simulation

The 3-D vascular model being at our disposal, the second step, aimed at a better understanding of the image features, and particularly its texture (Fig. 1), consists to simulate the physical process underlying the image formation. CT has been chosen due to its wide use and the flexibility it offers to control the image conditioning through its attached parameters (resolution and slice thickness for instance) which lead to different appearances of the structures under study. The main steps of CT acquisition modeling based on a simulated organ are depicted in Fig. 7. The results being illustrated on the vascular structure of the liver, some of its specific features related to contrast product tracking, will be briefly described.

A. Simulation of CT Scans

A cross-sectional slice of the organ has to be represented in the image. Each voxel of the model volume is associated with a density value so that the resulting 2-D image will display the usual CT numbers (the gray level in each pixel of the image is proportional to the CT number of the voxel in the appropriate position [27]). The first step consists to create a 3-D representation of the object to be displayed in the image. Some of the voxels of the slice are situated into a vessel or at their boundary (i.e., hence, the partial volume effect) but others are located in the parenchyma and no distinguishable vessel goes across them.

A mean density is allocated to the parenchyma voxels according to the class of macro-cells they belong to. Their density variations are taken into account to render the spatial fluctuations of micro-vessels (or capillaries): a random value following a Gaussian distribution is added to the mean density value. The density of the voxel intersecting partially a vessel is computed by weighting the respective volumes occupied by the blood and the parenchyma. Random noise can also be added to deal with heterogeneities of contrast medium.

One of the parameters of the CT acquisition model is the resolution of the simulated image. To set the size of the pixel, a zooming factor is applied to the corresponding tissue region, whose position is also calculated to coincide to the 3-D region of interest. The slice thickness is another parameter of the model. If the cross-sectional slice of the organ is thicker than a single voxel size, all densities of the voxels are aggregated at the same position but in the consecutive layers to obtain a 2-D density representation of the tissue.

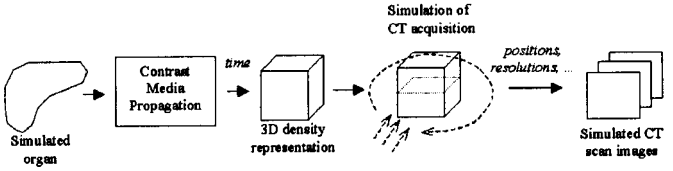

Fig. 7. CT scan-like images of simulated organ are acquired based on 3-D-density representation created at a given time moment, after injection and propagation of CM.

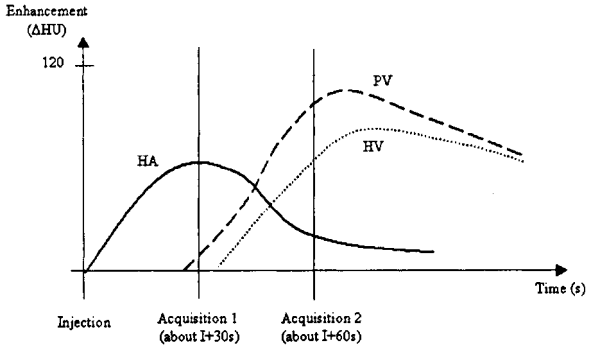

Fig. 8. Hepatic enhancement after injection (I) of a CM. CM first arrives in the HA, and after a delay in the Portal Vein (PV). The Hepatic Vein (HV) collects the blood from both HA and PV. Values of time and enhancement are approximate.

TABLE I
Model Parameters Used in the Simulation of Hepatic Vascular Network (Typical Values for a Normal Adult Liver, See [15] for More Details)

Model parameter	Hepatic artery	Portal vein	Hepatic vein
Blood pressure at the input P_{in} (mm Hg)	95	15	5
Blood pressure at the output P_{out} (mm Hg)	25	8	2
Wall thickness ratio (fraction of vessel radius)	0.2	0.1	0.1
Hepatic blood flow (ml/min)	400	800	1200
Size of the macro-cell (cm^3)		0.125	
Number of growth cycles		50	
Initial liver size (cm^3)		75	
Adult liver size (cm^3)		1500	
Number of macro-cells in the adult liver		~12000	

Based on the density 3-D map, the CT scan acquisition is carried out through the following steps.

- X-ray parallel projections are computed, using the Radon transform.
- Projections are filtered in the Fourier domain, by a filter with impulse response in $|\omega|$ (each Fourier coefficient is multiplied by its frequency).
- The back-projection is applied to reconstruct the image.

A more detailed description of the method used to simulate CT scan images is given in [18].

B. Modeling of Vessels Enhancement

In Section V-A, the CT scan simulation has been described, where a constant density (higher than the density of parenchyma) was attributed to all the voxels within the vessels. This situation anticipated the fact that a CM is injected

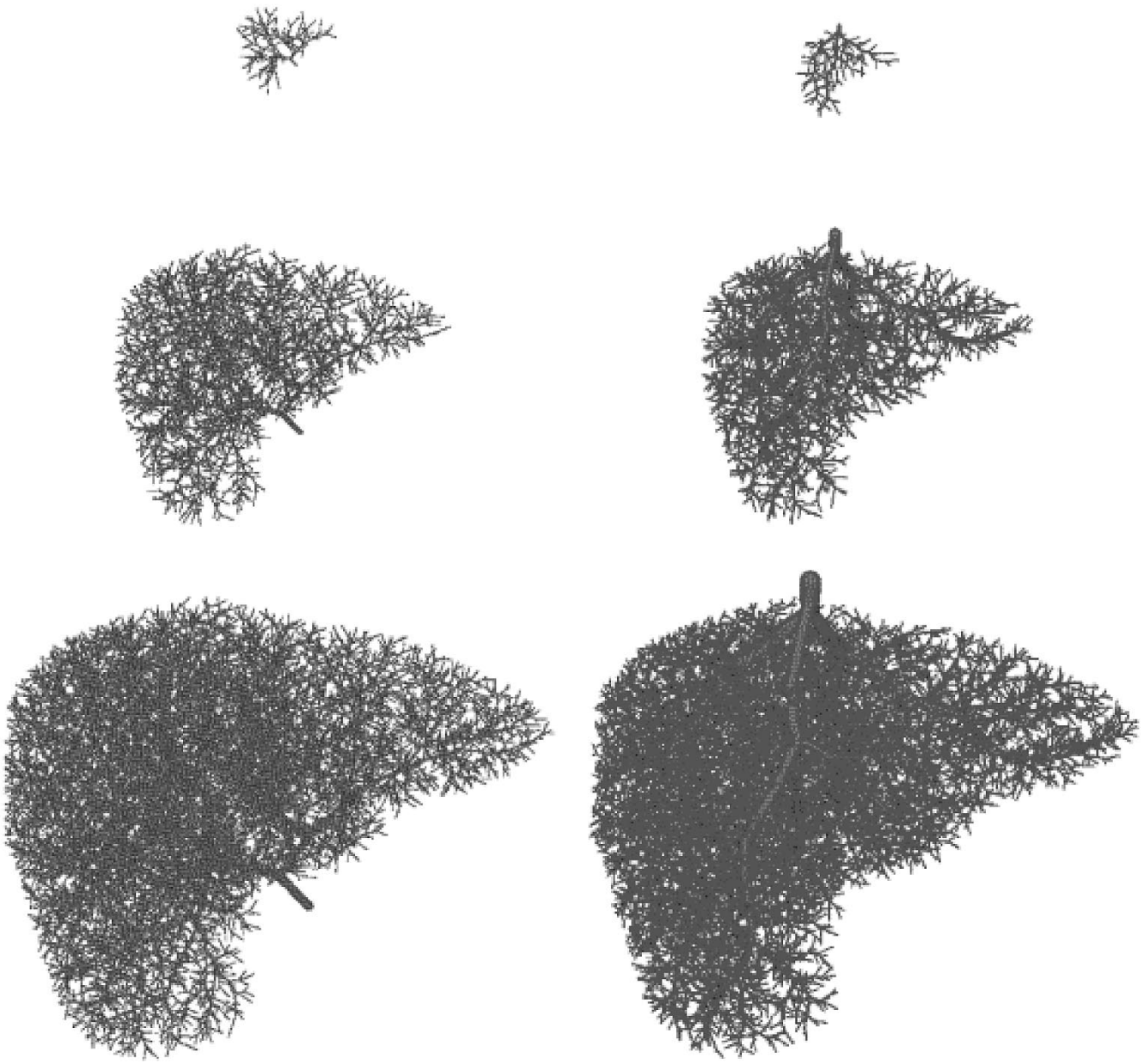

Fig. 9. Simulation of the growth of hepatic arterial (left column) and venous (right one) trees after 1, 25, 50 cycles (the main parameters are collected in Table I).

before performing a CT acquisition in order to enhance the vessels with respect to the parenchyma. In fact, in addition to the partial volume effect already mentioned, the amount of CM into a given vessel has to be taken into account. It should be emphasized that the contrast product propagation is a time-dependent process. In Fig. 8, the liver enhancement after injection of CM is schematically presented. First, the *hepatic artery* (HA) is filled by the CM. Then the CM arrives in the *portal vein* (PV) and it also appears in the *hepatic vein* (HV). The present model allows to simulate the CM injection in the arterial/portal tree and its propagation to the hepatic venous tree. The profile of the injection (i.e., duration and shape and also time-stamped delivery sequence) can easily be changed. The propagation of the CM within the capillary network is simplified and represented by a delay between HA/PV and HV following a Gaussian distribution.

VI. Results

The model was applied to simulate the growth of liver vascular structures. The hepatic vascular system is very specific, because it is made of three trees (Hepatic Arteries, Hepatic Veins and also Portal Veins). Two of these three trees can be simultaneously simulated by the model, taking into account their geometric and hemodynamic relations. The hepatic veins can be seen as the only output (it carries blood out of the liver, to the *vena cava* and then to the heart) and are here coupled either with the hepatic arteries or with the portal veins.

The main parameters used to illustrate the model behavior are defined in Table I. The 3-D bounding shape of the liver has been reconstructed from CT-scan images (Siemens Somaton, 120 slices with 1 mm thickness) after interactive delineation. The model was initialized with two trees consisting only of

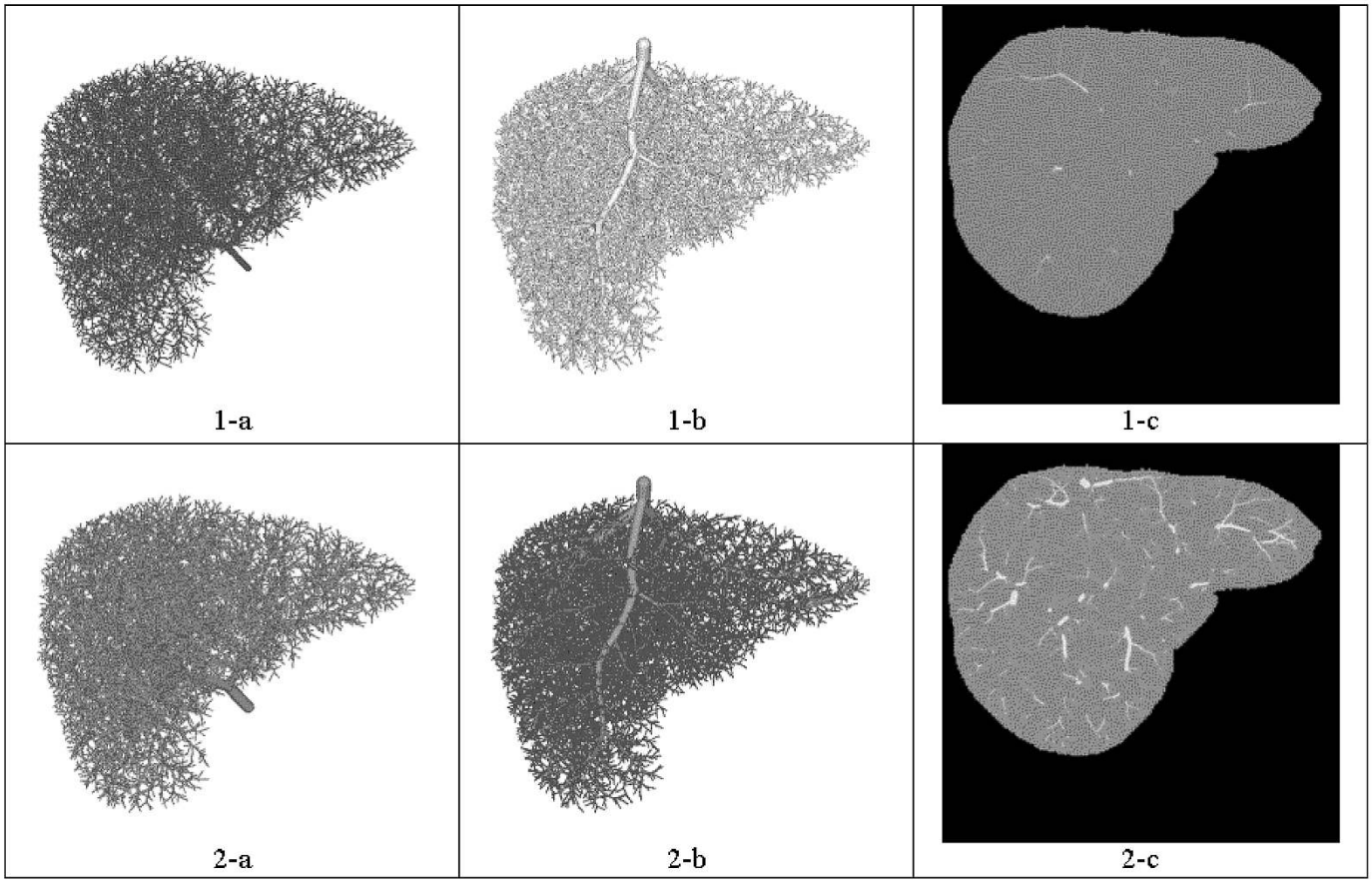

Fig. 10. Simulation of the CT scan images (the same position and acquisition parameters) at two time moments chosen from a temporal sequence, during liver enhancement (Fig. 8). 1) Acquisition time 1 (bolus only in the arterial tree): (a) 3-D representation of the injected arterial tree, (b) 3-D representation of hepatic venous tree, (c) CT slice simulation at time 1 (early phase = arterial phase). 2) Acquisition time 2 (bolus mainly in the portal and hepatic venous trees): (a) 3-D representation of the injected portal tree, (b) 3-D representation of injected hepatic venous tree, (c) CT slice simulation at time 2 (late phase = PV + HV).

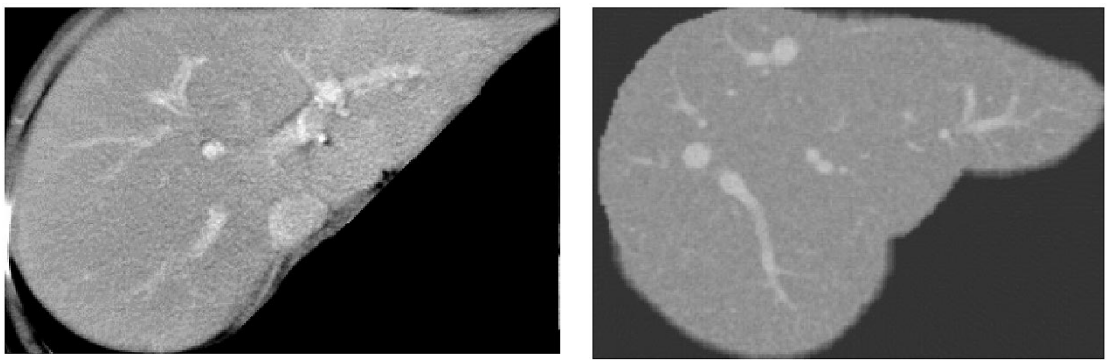

(a) (b)

Fig. 11. Comparison of (a) CT acquisition (portal phase—5 mm) with (b) simulated CT slice (portal phase—5 mm).

7 vessel segments. The geometry of this initial network was chosen based on anatomical data [28]. The structure of the largest vessels is kept the same for the HA or for the PV because they are effectively very similar in their main branches. The development of the intrahepatic vascular structures is shown in Fig. 9. Each tree is presented separately to enable a better visualization, but the two trees are physically connected. The simulation was performed on a PC (Pentium II 350-MHz, 512-MB RAM) and the adult hepatic vascular network (with about 12 000 perfusion sites) is obtained in about 5 hours.

During the propagation of a contrast medium, series of virtual CT scans can be collected, representing acquisitions at different times. The 3-D representation of the hepatic arteries and the hepatic veins, as well as the corresponding CT slices, are depicted in Fig. 10. Fig. 10(1) corresponds to a very early phase of a first CT acquisition where only the arterial tree is enhanced. This time instant is marked by "Acquisition 1" in Fig. 8. Fig. 10(2) shows the result of the simulation of a CT acquisition at a later phase when both portal and hepatic veins are enhanced. A visual comparison of a real CT acquisition is proposed in Fig. 11

which allows to show the realism of the model. These two images are acquired or synthesized with the same acquisition parameters (slice thickness = 5 mm, pixel size = 0.5 mm, portal time). The most important differences between these two images is due to the location of the main branches. Concerning the simulated images, this position depends on the initialization of the vascular trees (primary branches). Using segmented vessels from acquired images to start the growth should increase the similarity. The approach described in [29] could be adapted to extract the main vascular structures.

VII. Conclusion and Future Research

The above model-based approach to medical image analysis is aimed at a better understanding of image contents, for instance textural features. The methodology is made of a sequence of two modeling processes. The first one is a 3-D model of vascular tree, which allows us to simulate the growth of vascular networks (two connected trees without vessel intersection), following physiological rules (pressure, blood flow, and vascular density) and morphological boundary constraints, in normal or abnormal cases. The second step of the process consists to model the imaging device, the CT scan acquisitions, which offers the capability to vary its parameters (number of projections, resolution, thickness, contrast product injection, and acquisition time). The final step deals with the tissue characterization and has been already reported in [18]: classical methods of texture analysis (co-occurrence, gradients, and run-length) have been applied on images representing normal and hypervascularized tissues. In this study, a simplified method of arteries enhancement (the same density for all the vessels) was used. It has been shown that textural features can be used to discriminate the two kinds of tissue and that the resulting performance is dependent on the slice thickness.

A visual comparison in 3-D (with CT reconstruction of silicon cast) and in two dimensions (with *in vivo* acquisitions) as well as geometric and hemodynamic characterization have been carried out to evaluate the approach [15]. However, any model remains an approximation of reality and simplification have been made. For instance, the growth of tissues and vascular trees is a continuous and highly parallel process but it has been simulated in a sequential way and at discrete time cycles. The vessels have been assimilated to rigid tubes in which the blood flow is laminar: elasticity, pulsate flow, and turbulence could be also considered.

The model deals with macrovessels (larger than arterioles and veinules), while the microcirculation (tissue perfusion) is also of concern. Parenchyma is in fact made of microscopic vessels (capillaries) surrounded by tissue cells and it constitutes the place of vital exchanges between blood and tissue. These exchanges should be examined more precisely in order to be able to simulate the complete process of tissue enhancement after injection of contrast product, as well as pathological processes and their behavior over time or with respect to therapy.

As far as the image acquisition is concerned, many refinements could also be brought to the model. For example, in the CT scan modeling, parallel projection could be replaced by a conic one. Furthermore, any modality capable to provide insights into vascular diseases is candidate for such an approach like MRI or US imaging.

These perspectives show the generic character and the potential of the present work and motivate the on-going attempts. As such, however, a number of properties can be derived which have been only partially sketched in this paper.

References

[1] A. Bruno, R. Collorec, J. Bézy-Wendling, P. Reuzé, and Y. Rolland, "Texture analysis in medical imaging," in *Contemporary Perspectives in Three-dimensional Biomedical Imaging*, C. Roux and J. L. Coatrieux, Eds. Amsterdam, The Netherlands: IOS, 1997, pp. 133–164.

[2] M. E. Gottlieb, "Modeling blood vessels: A deterministic method with fractal structure based on physiological rules," in *Proc. Int. Conf. IEEE Engineering in Medicine and Biology Society*, vol. 12, 1990, pp. 1386–7.

[3] F. Nekka, S. Kyriacos, C. Kerrigan, and L. Cartilier, "A model of growing vascular structures," *Bull. Math. Biol.*, vol. 58, no. 3, pp. 409–24, 1996.

[4] V. Meier, "Realistic Visualization of Abdominal Organs and its Application in Laparoscopic Surgery Simulation," Ph.D. dissertation, Swiss Fed. Inst. Technol., Zurich, 1999.

[5] W. Schreiner and P. F. Buxbaum, "Computer optimization of vascular trees," *IEEE Trans. Biomed. Eng.*, vol. 40, pp. 482–91, May 1993.

[6] W. Schreiner, F. Neumann, M. Neumann, A. End, and M. Müller, "Structural quantification and bifurcation symmetry in arterial tree models generated by constrained constructive optimization," *J. Theor. Biol.*, vol. 180, pp. 161–174, 1996.

[7] W. Schreiner, F. Neumann, M. Neumann, A. End, and S. Roedler, "Anatomical variability and functional ability of vascular trees modeled by constrained constructive optimization," *J. Theor. Biol*, vol. 187, pp. 147–158, 1997.

[8] A. R. A. Anderson and M. A. J. Chaplain, "Continuous and discrete mathematical models of tumor-induced angiogenesis," *Bull. Math. Biol.*, vol. 60, pp. 857–900, 1998.

[9] J. Lefevre, "A theoretical study of the relationships between fractal complexity and functional efficiency in the pulmonary arterial tree," in *Annu. Int. Conf. IEEE Engineering in Medicine and Biology Society*, vol. 13, 1991, pp. 2198–2199.

[10] ——, "Fractal models of vascular trees: Current status and potential developments," in *Annu. Int. Conf. IEEE Engineering in Medicine and Biology Society*, vol. 3, Paris, France, 1992, pp. 986–987.

[11] R. W. Glenny and H. T. Robertson, "A computer simulation of pulmonary perfusion in three dimensions," *J. Appl. Physiol.*, vol. 79, no. 1, pp. 357–69, 1995.

[12] J. C. Parker, C. B. Cave, J. L. Ardell, C. R. Hamm, and S. G. Williams, "Vascular tree structure affects lung blood flow heterogenity simulated in three dimensions," *J. Appl. Physiol.*, vol. 83, no. 4, pp. 1370–82, 1997.

[13] R. Karch, F. Neumann, M. Neumann, and W. Schreiner, "A three-dimensional model for arterial tree representation, generated by constrained constructive optimization," *Comput. Biol. Med.*, vol. 29, pp. 19–38, 1999.

[14] ——, "Staged growth of optimized arterial model trees," *Ann. Biomed. Eng.*, vol. 28, pp. 495–511, 2000.

[15] J. Bézy-Wendling and A. Bruno, "A 3-D dynamic model of vascular trees," *J. Biological Syst.*, vol. 7, no. 1, pp. 11–31, 1999.

[16] Y. Rolland, J. Bézy-Wendling, R. Duvauferrier, and A. Bruno, "Modeling of the parenchymous vascularization and perfusion," *Investigat. Radiol.*, vol. 34, no. 3, pp. 171–175, 1999.

[17] Y. Rolland, J. Bézy-Wendling, R. Duvauferrier, and J. L. Coatrieux, "Slice simulation from a model of the parenchymous vascularization to evaluate texture features," *Investigat. Radiol.*, vol. 34, no. 3, pp. 181–184, 1999.

[18] J. Bézy-Wendling, M. Kretowski, Y. Rolland, and W. Le Bidon, "Toward a better understanding of texture in vascular CT scan simulated image," *IEEE Trans. Biomed. Eng.*, vol. 48, pp. 120–124, Jan. 2001.

[19] R. J. Goss, *The Strategy of Growth, Control of Cellular Growth in Adult Organizms*, H. Teir and T. Rytömaa, Eds. New York: Academic, 1967.

[20] M. Zamir, "Optimality principles in arterial branching," *J. Theor. Biol.*, vol. 62, pp. 227–251, 1976.

[21] A. Kamiya and T. Togawa, "Optimal branching structure of the vascular trees," *Bull. Math. Biophys.*, vol. 34, pp. 431–438, 1972.

[22] D. L. Cohn, "Optimal systems: I. The vascular system," *Bull. Math. Biophys.*, vol. 16, pp. 59–74, 1954.

[23] O. Hudlicka, M. B. Brown, and S. Egginton, "Angiogenesis: Basic concepts and methodology," in *An Introduction to Vascular Biology*, A. Halliday, B. Hunt, L. Poston, and M. Schachter, Eds. Cambridge, U.K.: Cambridge Univ. Press, 1998, pp. 3–19.

[24] C. D. Murray, "The physiological principle of minimum work applied to the angle of branching arteries," *J. Gen. Physiol*, vol. IX, no. 835, 1925–26.

[25] R. Rosen, *Optimality Principles in Biology, the Vascular System*. London, U.K.: Butterworths, 1967, pp. 41–60.

[26] M. Kretowski, Y. Rolland, J. Bézy-Wendling, and J. L. Coatrieux, "Fast algorithm for 3-D vascular tree modeling," *Comput. Methods Programs Biomed.*.

[27] G. T. Herman, "Image reconstruction from projections, the fundamentals of computerized tomography," *Comput. Sci. Appl. Math.*, 1980.

[28] J. E. Healey, P. C. Schroy, and R. Sorensen, "The intrahepatic distribution of the hepatic artery in man," *The J. Int. College Surgeons*, vol. XX, no. 2, Aug. 1953.

[29] D. Selle, W. Spindler, B. Preim, and H. O. Peitgen, "Mathematical methods in medical imaging: Analysis of vascular structures for liver surgery planning," in *Mathematics Unlimited—2001 and Beyond*. Berlin, Germany: Springer-Verlag, 2000, pp. 1039–1059.